nature synthesis

Article

https://doi.org/10.1038/s44160-025-00759-x

A three-step strategy for the conversion of pyridines into benzonitriles

Received: 29 August 2024

Accepted: 3 February 2025

Published online: 7 March 2025

Check for updates

Reyhan Güdük[1], Niklas Kehl[1,5], Chiara Stavagna[1,5], Michael J. Tilby[2], Oliver Turner[3], Alessandro Ruffoni[1] ✉, Henry P. Caldora[4] ✉ & Daniele Leonori[1] ✉

Bioisosteric replacement is a key strategy in drug discovery. Although modifying peripheral functionalities is relatively straightforward, substituting core ring structures often demands a complete synthetic redesign. Substituting benzenes with pyridines is often pursued because the nitrogen atom in pyridine can enhance biological potency and metabolic stability. Conversely, replacing pyridines with benzenes, particularly benzonitriles, can also be of value. Benzonitriles are similarly polarized to pyridines and can effectively mimic their hydrogen-bond acceptor properties. Here we introduce a strategy for converting pyridines into benzonitriles. The method uses a three-step protocol, beginning with pyridine *N*-oxidation, followed by photochemical deconstruction in the presence of an amine. This sequence produces a nitrile-containing butadiene, which then undergoes a formal Diels–Alder cycloaddition with alkynes and alkenes to construct the benzonitrile ring. This methodology provides a retrosynthetic tactic for the preparation of benzonitriles from pyridine-based starting materials and enables direct, modular late-stage diversification of drug molecules.

Bioisosteric replacement is a pivotal strategy extensively used during critical phases of drug discovery campaigns[1]. At the lead optimization stage, it is often used in library generation for both hit expansion and structure–activity relationship (SAR) studies. Additionally, it is an effective method to circumvent patent protection, something generally referred to as 'scaffold hopping'[2].

Although the bioisosteric replacement of specific peripheral functional groups can be performed in a modular and programmable fashion (for example, via amidation, cross-coupling or C–H activation), the bioisosteric replacement of a core ring structure within a bioactive molecule often necessitates a ground-up redesign of the entire synthetic sequence. This endeavour is necessarily time consuming and costly[3]. Consequently, reactions enabling modular late-stage 'ring replacement' allow for rapid diversification in retrosynthetically unconventional manners. Such processes are in high demand yet remain rare due to the considerable synthetic challenges they pose[4–16].

A highly sought-after ring replacement in medicinal chemistry involves substituting benzene with pyridine because the incorporation of a nitrogen atom in the arene can often boost biological potency. This phenomenon, frequently observed and now termed the 'necessary nitrogen effect', is mainly due to the inherent metabolic stability imparted by the nitrogen atom (pyridine is more difficult to oxidize than benzene) and the potential for hydrogen-bond interactions through its lone pair of electrons[17–21].

However, given the ubiquity of pyridine-containing bioactive material[22], the opposite direction of ring replacement, namely, pyridine to benzene, can also provide many opportunities for SAR studies (Fig. 1a). Among the various types of benzenoid systems, benzonitriles hold a privileged position. A nitrile group can effectively

[1]Institute of Organic Chemistry, RWTH-Aachen University, Aachen, Germany. [2]School of Chemistry, University of Bristol, Bristol, UK. [3]The DISC, Cambridge, UK. [4]Department of Chemistry, University of Manchester, Manchester, UK. [5]These authors contributed equally: Niklas Kehl, Chiara Stavagna. ✉e-mail: alessandro.ruffoni@rwth-aachen.de; henry.caldora@postgrad.manchester.ac.uk; daniele.leonori@rwth-aachen.de

https://doi.org/10.1038/s44160-025-00759-x

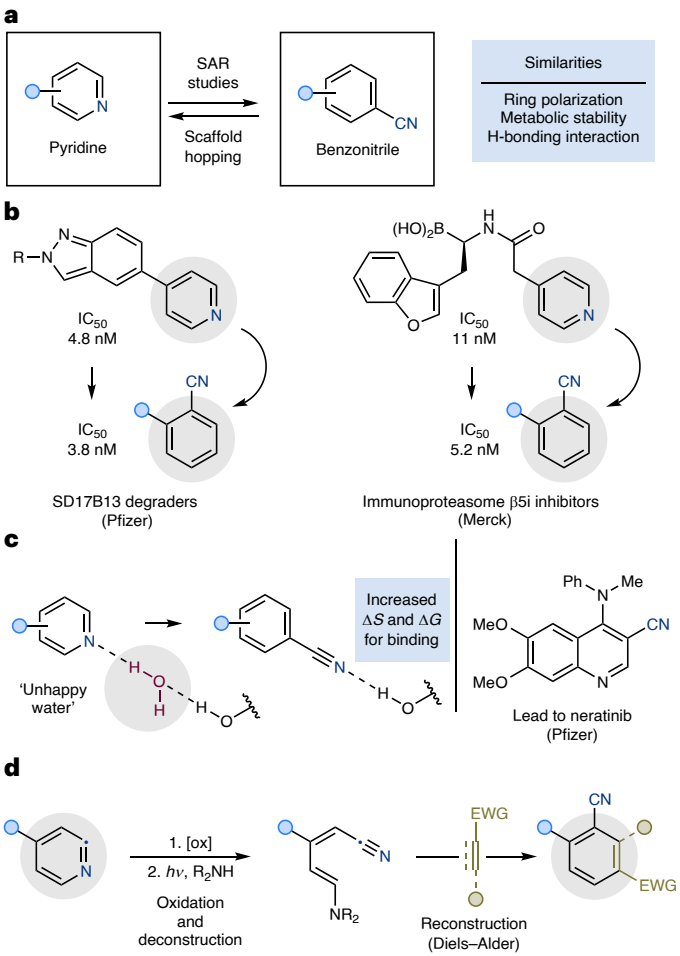

Fig. 1 | The 'ring replacement' of pyridines into benzonitriles. a, The bioisosteric replacement of pyridines with benzonitriles is often used in medicinal chemistry studies[23,28]. **b**, 2-Substituted benzonitriles are powerful bioisosteric replacements for 4-substituted pyridines[29–33]. **c**, The replacement of the pyridine nitrogen atom with a 'C–CN' unit can improve biological activity by displacement of 'unhappy water' molecules[27,35,36]. **d**, This work provides a three-step method for the conversion of 4-substituted pyridines into 2-substituted benzonitriles. EWG, electron-withdrawing group; IC_{50}, half-maximal inhibitory concentration; [ox], oxidation.

polarize the aromatic ring similarly to pyridine, thereby enhancing metabolic stability in most cases[23–27]. In practice, two main types of pyridine-to-benzonitrile replacements have demonstrated strong potential and consequent applicability in medicinal chemistry. First, 2-substituted benzonitriles have been identified as effective bioisosteres for 4-substituted pyridines[23,28–33] (Fig. 1b). This is particularly important given that the 4-substituted pyridine motif appears in nearly one-third of all US Food and Drug Administration (FDA)-approved drugs featuring this azine core[22]. Furthermore, another commonly used replacement involves substituting the pyridine nitrogen atom with a 'C–CN' unit because the nitrile group can mimic the pyridine hydrogen-bond acceptor ability[34] (Fig. 1c). This approach has been particularly useful when one bridging H_2O molecule is involved in the binding of a bioactive pyridine with its biological target[27]. This bioisosteric replacement can effectively displace the 'unhappy water' from the interaction site, thereby reducing the entropy of binding[35,36]. Such a strategy has often been pivotal in the development of commercial drugs such as neratinib and bosutinib from Pfizer or other highly active molecules such as a p38 inhibitor under development by Bristol-Myers Squibb[27,37–39].

Overall, designing a synthetic strategy for pyridine-to-benzonitrile replacement might be a useful tool for SAR studies and scaffold hopping purposes. Here we present a photochemical strategy that converts 4-substituted pyridines into 2-substitute benzonitriles in just three steps (Fig. 1d). The method requires initial pyridine *N*-oxidation, for photochemical deconstruction into a nitrile-containing linear intermediate. This species is then rearomatized into the corresponding 2-substituted benzonitrile via Diels–Alder cycloaddition with various dienophiles. This process leverages the externalization of the pyridine nitrogen atom into the nitrile functionality, thereby bypassing the need for toxic cyanide sources typically used in transition-metal-mediated cyanation strategies[40].

Results and discussion

Design plan

The design of our three-step process is based on a strategic photochemical pyridine deconstruction step to form an acyclic-nitrile-containing intermediate (Fig. 2a). For this step to occur, initial pyridine activation is required by *N*-oxidation generally with *meta*-chloroperoxybenzoic acid (*m*CPBA) (step a, **I** → **II**). Pleasingly, many pyridine-*N*-oxides are also commercially available, thus reducing the pyridine-to-benzonitrile replacement to effectively two steps.

In the key photochemical deconstruction event, one pyridine endocyclic C–N unit is transformed into a nitrile group, while creating a dienic structure (**IX**) capable of participating in ring-constructing reactions, such as Diels–Alder cycloaddition, with a second synthon (**IX** + **X** → **XI**)[41–46]. For the deconstruction step, we drew inspiration from the pioneering work of Buchardt, Lohse and Albini showing that 4-substituted pyridine-*N*-oxides, upon irradiation with a mercury lamp in the presence of an amine, undergo a photochemical ring opening sequence producing an aminopentadienenitrile intermediate. However, this reactivity proved low yielding, giving the desired product alongside 2-formyl pyrrole derivatives and tarring under the stated conditions[47–53]. Mechanistically, it has been postulated that, upon irradiation, **II** populates its S_1 state that has π,π^* character (step b). This excited state species would then initiate an oxygen-atom insertion to provide a transient oxaziridine (step c, **IV**)[54], evolving by electrocyclic 6π ring opening into a 1,2-oxazipine **V** (step d)[55]. At this point, a second photon absorption event would deliver the S_1-**VI** (step e) from where a triplet nitrene can be extruded (step f, **VI** → **VII**)[56]. Exploitation of the intrinsic acidity of the α-nitrene C(sp^2)–H bond in **VII** allows for deprotonation to generate the nitrile functionality in **VIII** (step g)[57–60]. The resulting enolatepentadienenitrile **VIII** can then condense with an amine to furnish the desired aminopentadienenitrile **IX** (step h).

For the third and final step of our strategy, we postulated that **IX** would be sufficiently electron-rich to undergo [$4\pi_s + 2\pi_s$] Diels–Alder cycloaddition followed by concomitant aromatization with a suitably electron-deficient dienophile **X** (step i).

Overall, the successful implementation of this synthetic design would generate a benzonitrile species **XI** in which the nitrogen atom has been externalized and converted into a nitrile functionality, while the pyridine substituent at the 4-position has been translated, in a programmable and regioselective manner, to its 2-position. Moreover, the introduction of a difunctionalized dienophile at the cycloaddition stage can potentially enable simple access to 1,2,3,4-tetrasubstituted aromatics, which are challenging synthetic derivatives due to their sterically congested cores[61].

Reaction development and understanding

We proceeded with the optimization of the key pyridine deconstructive step by using the commercial 4-BnO-pyridine-*N*-oxide **1a** (Fig. 2b). Pleasingly, irradiation (λ = 310 nm) of **1a** and morpholine (10 equiv.) in CH_3CN solvent at room temperature for 15 h provided diene **1** in high yield (entry 1). The use of lower amounts of morpholine (entry 2)

https://doi.org/10.1038/s44160-025-00759-x

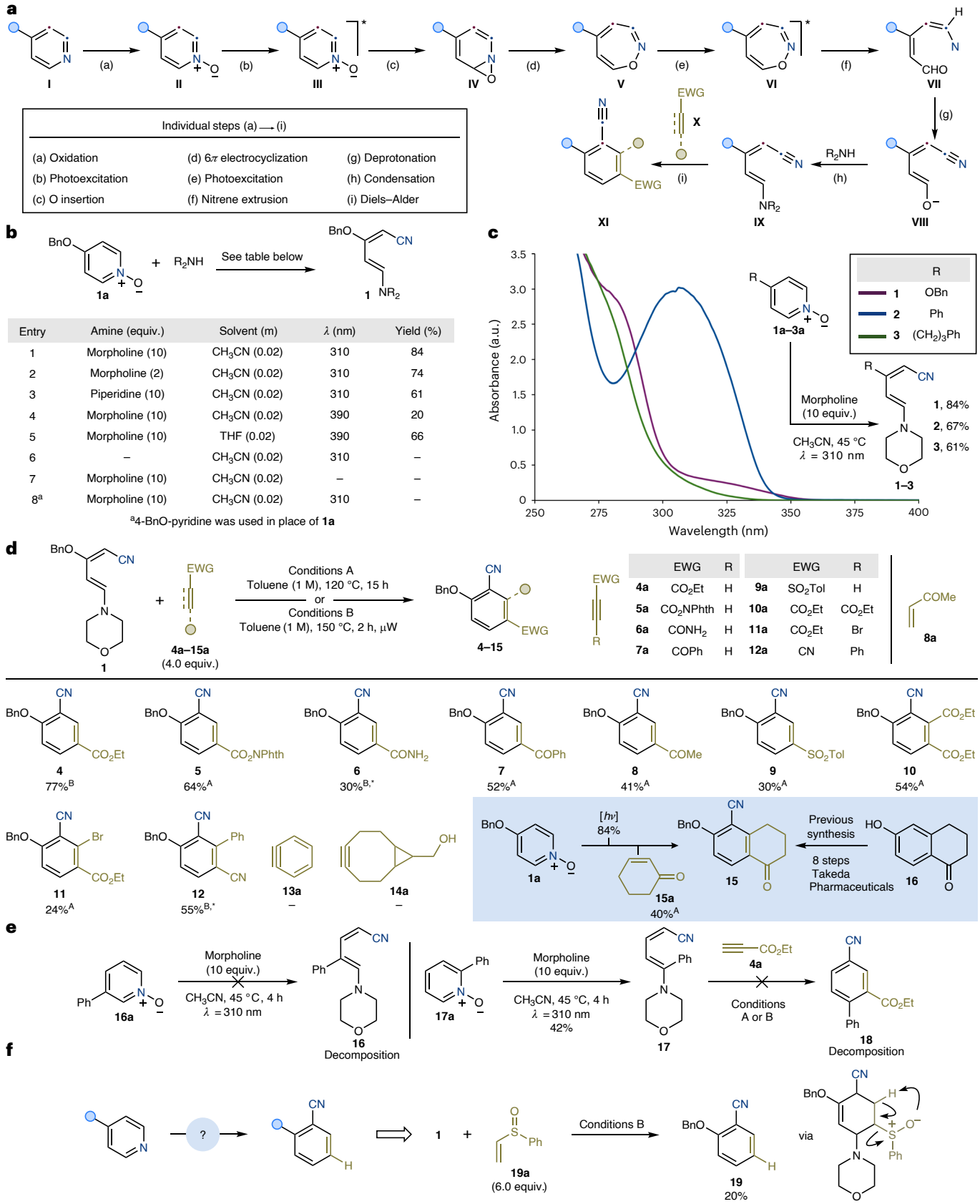

Entry	Amine (equiv.)	Solvent (m)	λ (nm)	Yield (%)
1	Morpholine (10)	CH_3CN (0.02)	310	84
2	Morpholine (2)	CH_3CN (0.02)	310	74
3	Piperidine (10)	CH_3CN (0.02)	310	61
4	Morpholine (10)	CH_3CN (0.02)	390	20
5	Morpholine (10)	THF (0.02)	390	66
6	–	CH_3CN (0.02)	310	–
7	Morpholine (10)	CH_3CN (0.02)	–	–
8[a]	Morpholine (10)	CH_3CN (0.02)	310	–

[a]4-BnO-pyridine was used in place of **1a**

	EWG	R		EWG	R
4a	CO_2Et	H	**9a**	SO_2Tol	H
5a	CO_2NPhth	H	**10a**	CO_2Et	CO_2Et
6a	$CONH_2$	H	**11a**	CO_2Et	Br
7a	COPh	H	**12a**	CN	Ph

4 77%[B] **5** 64%[A] **6** 30%[B,*] **7** 52%[A] **8** 41%[A] **9** 30%[A] **10** 54%[A]
11 24%[A] **12** 55%[B,*] **13a** – **14a** –
15 40%[A]
Previous synthesis: 8 steps Takeda Pharmaceuticals → **16**

Fig. 2 | Development and mechanistic understanding of a pyridine-to-benzonitrile replacement. a, Mechanistic pathway for the three-step conversion of 4-substituted pyridines into 2-substituted benzonitriles. **b**, Reaction development for the photochemical conversion of **1a** into **1**. **c**, Ultraviolet–visible absorption spectroscopy studies. **d**, Diels–Alder cycloaddition scope and applications. **e**, Current limitations. **f**, Use of (vinylsulfinyl)benzene as dienophile enables access to 2-substitued benzonitriles without substituents at C5. Superscripts A and B indicate reactions performed using conditions A and B, respectively. *See Supplementary Information, section 11.2, for further details. Bn, benzyl; λ, irradiation wavelength; Phth, phthalimide

or piperidine as the amine (entry 3) successfully delivered **1** albeit in slightly diminished yields.

Ultraviolet–visible absorption spectroscopy analysis on **1a** revealed high absorption in the 280–330 nm region with a tail reaching the near-visible region (Fig. 2c). However, utilization of purple light-emitting diodes (λ = 390 nm) resulted in low conversion in the deconstructive process (entry 4). Interestingly, we noticed a considerable solvochromic effect, and in tetrahydrofuran, the absorption profile of **1a** showed a notable bathochromic (red) shift, which in turn enabled the use of lower-energy light sources for the conversion into **1** (entry 5) (Supplementary Information). Control experiments in the absence of either morpholine (entry 6) or light irradiation (entry 7) or using 4-BnO-pyridine in place of the *N*-oxide **1a** (entry 8) resulted in no product formation.

Because this photochemical event is intrinsically reliant on the absorption profile of the various pyridine-*N*-oxide reagents, we quickly evaluated other derivatives featuring different electronic perturbations of the azine ring. In particular, 4-Ph and 4-alkyl derivatives **2a** and **3a** display a markedly lower absorption profile, but using λ = 310 nm we obtained the desired dienes **2** and **3** in good yields (Fig. 2c).

With a strategy for pyridine-*N*-oxide deconstruction in place, we then focused our attention on the following rearomatization step via Diels–Alder cycloaddition (Fig. 2d). This was initially performed on isolated diene **1**, which was routinely prepared on up to 5-mmol scales using our aforementioned photochemical ring-opening methodology. Although the supplementary material describes all optimization efforts using ethyl propiolate **4a** (Supplementary Information, section 4, and Supplementary Tables 10–14), we identified two simple thermal conditions using toluene as the solvent. In general, reactive dienophiles could be engaged at 120 °C (conditions A), whereas less-reactive ones required more forcing conditions, which were met with the use of a standard microwave apparatus (conditions B). Under these conditions, we successfully accessed benzonitriles **4**–**15** featuring *meta*-ester (**4** and **5**), primary amide (**6**), ketone (**7** and **8**) and sulfone (**9**) functionalities. It is interesting to note that the cycloaddition does not require the use of an alkyne dienophile as **8** was obtained using Me-vinyl-ketone **8a**. In this case, we propose that the cycloadduct intermediate undergoes morpholine elimination followed by aromatization by hydride transfer to the enone (Supplementary Information, section 12, and Supplementary Fig. 15). The formation of **5** is also synthetically noteworthy as the redox-active ester functionality can now be used in several radical-based cross-coupling manifolds for further functionalization[62–64]. Disubstituted alkynes were screened next and enabled access to tetrasubstituted aromatics with additional ester (**10**), bromine (**11**) and aryl (**12**) substituents. In terms of limitations, we did not succeed in engaging benzyne **13a** and the 'click chemistry' alkyne **14a** in the process. Preliminary computational studies indicated that the lack of a functionality on the alkyne of **14a** inhibits reactivity, while the finding for **13a** is probably a consequence of the high reactivity of benzyne (Supplementary Information, section 12, and Supplementary Fig. 41).The retrosynthetic opportunity that this approach might provide for the preparation of functional materials was demonstrated by the synthesis of tetralone **15**. This species has been recently patented by Takeda Pharmaceuticals as an intermediate in the synthesis of an API targeting the β-adrenoceptor[65,66]. Interestingly, its preparation was achieved using an eight-step synthetic route starting from phenol **16**. The unusual tactic introduced by our methodology simplified its preparation, shortening it to just two steps using commercial **1a** and **15a**.

A key observation in terms of limitations was that it could not be extended to 3- and 2-substituted pyridine-*N*-oxides such as **16a** and **17a** (Fig. 2e). In the case of **16a**, photochemical ring opening resulted in a complex mixture of products, possibly owing to the instability of its corresponding nitrene intermediate. By contrast, **17a** underwent efficient ring opening; however, the following cycloaddition with diene **17** could not be achieved because it led to extensive decomposition.

At the moment, our strategy enables the conversion of 4-substituted pyridines into 2-substituted benzonitriles with an additional electron-withdrawing substituent placed at C5. Although this group is necessary to favour the Diels–Alder step, it would be synthetically valuable to identify conditions to access C5-unsubstituted derivatives (Fig. 2f). This proposal would require a challenging cycloaddition step with gaseous acetylene. Hence, we decided to identify a potential synthon acting effectively as an acetylene surrogate. Specifically, we were pleased to identify that the use of (vinylsulfinyl)benzene **19a** as the dienophile led to the direct formation of **19** in 20% yield. We believe the initial sulfoxide-containing cycloadduct undergoes a tandem E_i-type elimination followed by aromatization by morpholine elimination[67,68].

The final cycloaddition event has not been studied before, and therefore we initiated a computational study with **1** and methyl propiolate (**I**) as the model partners (Fig. 3a). After a detailed conformational search of possible intermediates and transition states (Supplementary Information, section 12, and Supplementary Figs. 25 and 26) we found that the lowest-energy conformation of **1** has a *s-trans* arrangement. However, the lowest-energy transition states located for cycloaddition with **I** proceed through an *s-cis* conformation ($\Delta G^{\ddagger}$ = 38.1 kcal mol^{-1}), although the penalty of **1** adopting this reactive conformation is ΔG° = 2.7 kcal mol^{-1}. Considering the whole ensemble of feasible transition state structures of **1** reacting with **A**, it is noted that all occurred with a key $r(C_3–C_4)$ bond distance >2.92 Å and a much shorter $r(C_1–C_2)$ averaging 1.95 Å. This suggests the process occurs via an energetically concerted, highly asynchronous Diels–Alder process to give **C** that can eliminate morpholine to **D** or a more complex mechanism potentially through a stepwise process, potentially via intermediate **B**.

To understand the underlying physical contribution, we applied a distortion-interaction analysis to a model transition state primed for a concerted addition [69–73], which revealed that for this system the distortion energy is over twice the interaction energy ($\Delta E^{\ddagger}_{dis}$ = 30.7 kcal mol^{-1} and $\Delta E^{\ddagger}_{int}$ = 11.9 kcal mol^{-1}) (Fig. 3b). However, if the transition state is constrained to a more synchronous Diels–Alder type reactivity ($r(C_1–C_2)$ = 2.10 Å and $r(C_3–C_4)$ = 2.35 Å) a slight increase in interaction energy is observed ($\Delta E^{\ddagger}_{int}$ = 15.7 kcal mol^{-1}) but this does not compensate for the additional distortion ($\Delta E^{\ddagger}_{dis}$ = 38.1 kcal mol^{-1}). These findings further suggest that a synchronous Diels–Alder reaction does not provide sufficient energetic gains because it leads to a notable increase in strain.

The exemplar transition state was further studied with an analysis inspired by the work of Wheeler[74–77], in which the substituents were individually removed and capped with a hydrogen atom to discern their specific effects (Fig. 3c). These data point towards the -CN and -OBn groups contributing to the transition state through destabilizing interactions ($\Delta\Delta E^{\ddagger} < 0$ and $\Delta\Delta E^{\ddagger}_{int} > 0$) with minimal additional strain. This effect is offset by the morpholine and carboxylate groups, which now predominantly act to stabilize the transition state through the interaction term ($\Delta\Delta E^{\ddagger} > 0$ and $\Delta\Delta E^{\ddagger}_{int} < 0$). Overall, this analysis suggests the key strain energy associated with the transition state is intimately associated to its distorted six-membered-ring core with minimum impact from the various substituents.

Further analysis of the transition state revealed the presence of charge-transfer from the diene to the alkyne ($\Delta CT^{\ddagger} = -0.33e$). This can potentially be explained through the formation of a zwitterionic intermediate **B** undergoing cyclization to **C**. Our analysis suggested this process to be barrierless, hence potentially involving an 'entropic dynamic intermediate'[78,79]. To provide insights into this, we calculated intrinsic bonding orbitals[80,81] along the intrinsic reaction coordinates, which provide an intuitive way to understand the flow of electrons throughout the reaction, depicted on an ideal path along the More

https://doi.org/10.1038/s44160-025-00759-x

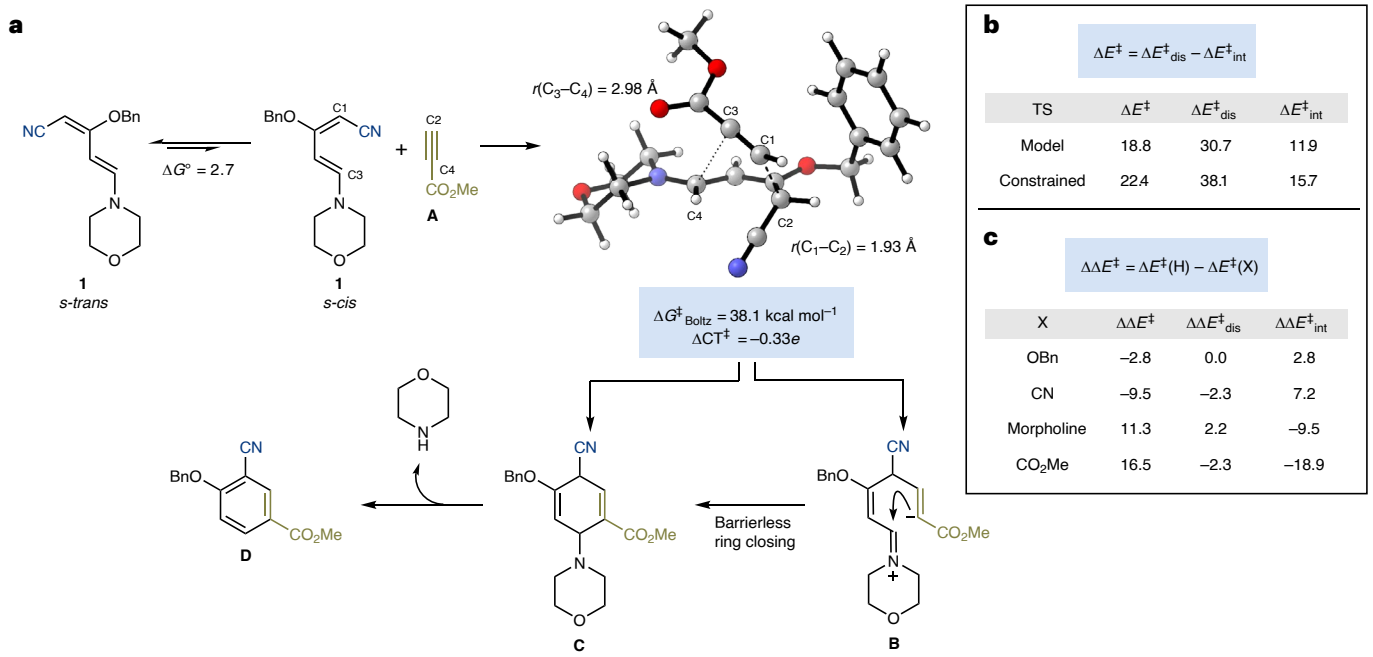

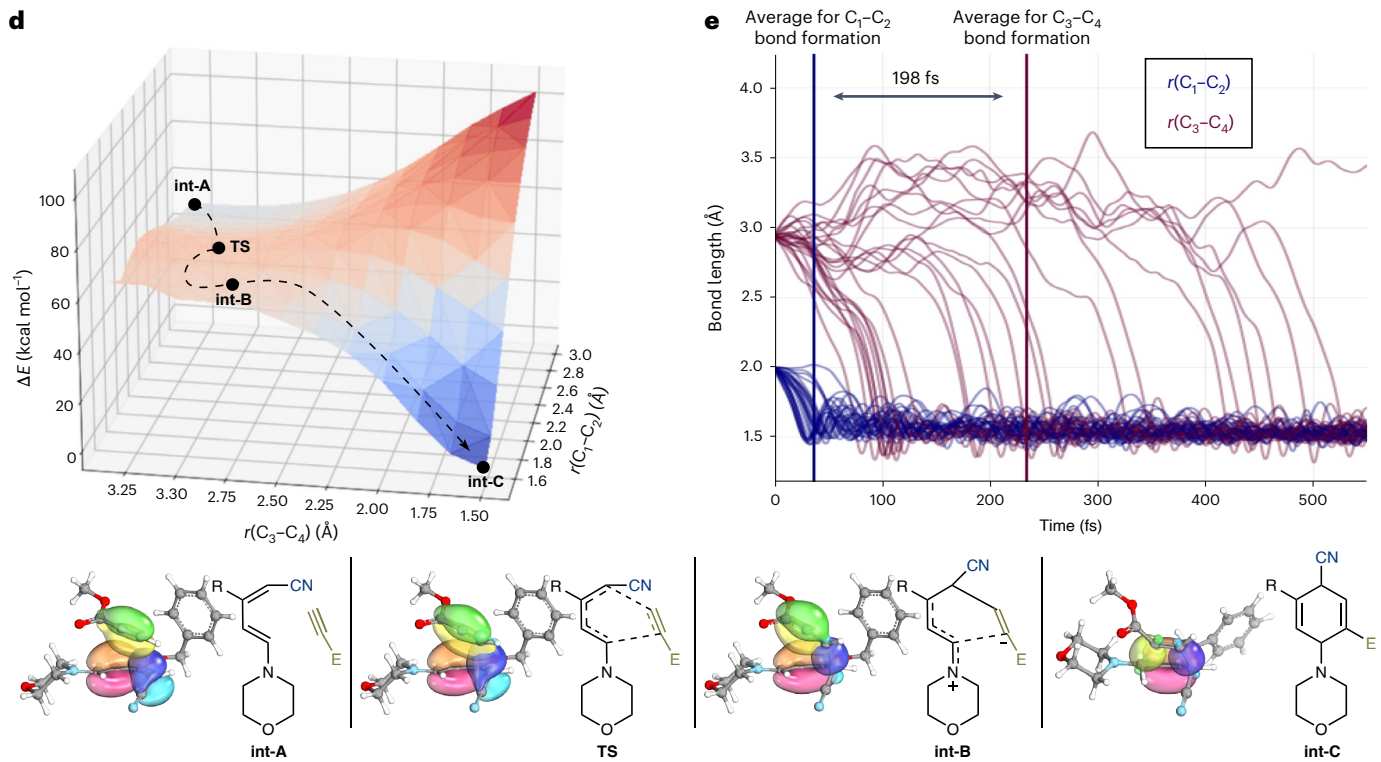

Fig. 3 | Computational studies for the proposed benzonitrile-forming cycloaddition. a, Proposed mechanism for formal cycloaddition. **b**, Distortion-interaction analysis conducted on an example transition state and a species with constrained bond lengths. **c**, Effects of substituents on the example transition state by their removal and capping with a hydrogen atom at the transition state geometry. Energy values in **b**,**c** are displayed in kcal mol^{-1}. **d**, More O'Ferrall–Jencks plot for a truncated system of the model transition state (CPCM(Toluene)-M06-2X/ma-def2-SVP), with an idealized reaction path. **e**, Analysis of Born–Oppenheimer molecular dynamics (CPCM(Toluene)-M06-2X/ma-def2-SVP), initiated from the truncated transition state, examining the time taken for the key bond formation. General method: SMD(Toluene)-M06-2X/ma-def2-QZVPP/CPCM(Toluene)-M06-2X/ma-def2-SVP. Orbitals: SMD(Toluene)-M06-2X/def2-TZVP/CPCM(Toluene)-M06-2X/ma-def2-SVP. Molecular dynamics: CPCM(Toluene)-M06-2X/ma-def2-SVP. E, CO_2Me; R, OBn; TS, transition state; for 3D structures, grey atoms are carbon, white hydrogen, red oxygen and blue nitrogen.

O'Ferrall–Jencks plot for a model system[82] (Fig. 3d). The intrinsic bonding orbital at the beginning of the reaction clearly indicates three π-bonds delocalized by their neighbouring environment (**int-A**); on progressing to the transition state two π-bonds spatially change with one converting to a σ-bond and the other a π-lone pair (**TS**). This is again in stark contrast to a standard Diels–Alder reactivity in which the other π-bond is involved to form a second σ-bond. This finding further reinforces the likelihood that even when the alkyne is aligned with the diene, the cycloaddition progresses through a stepwise zwitterionic entropic intermediate (**TS** → **int-B** → **int-C**). Therefore, to determine whether the

https://doi.org/10.1038/s44160-025-00759-x

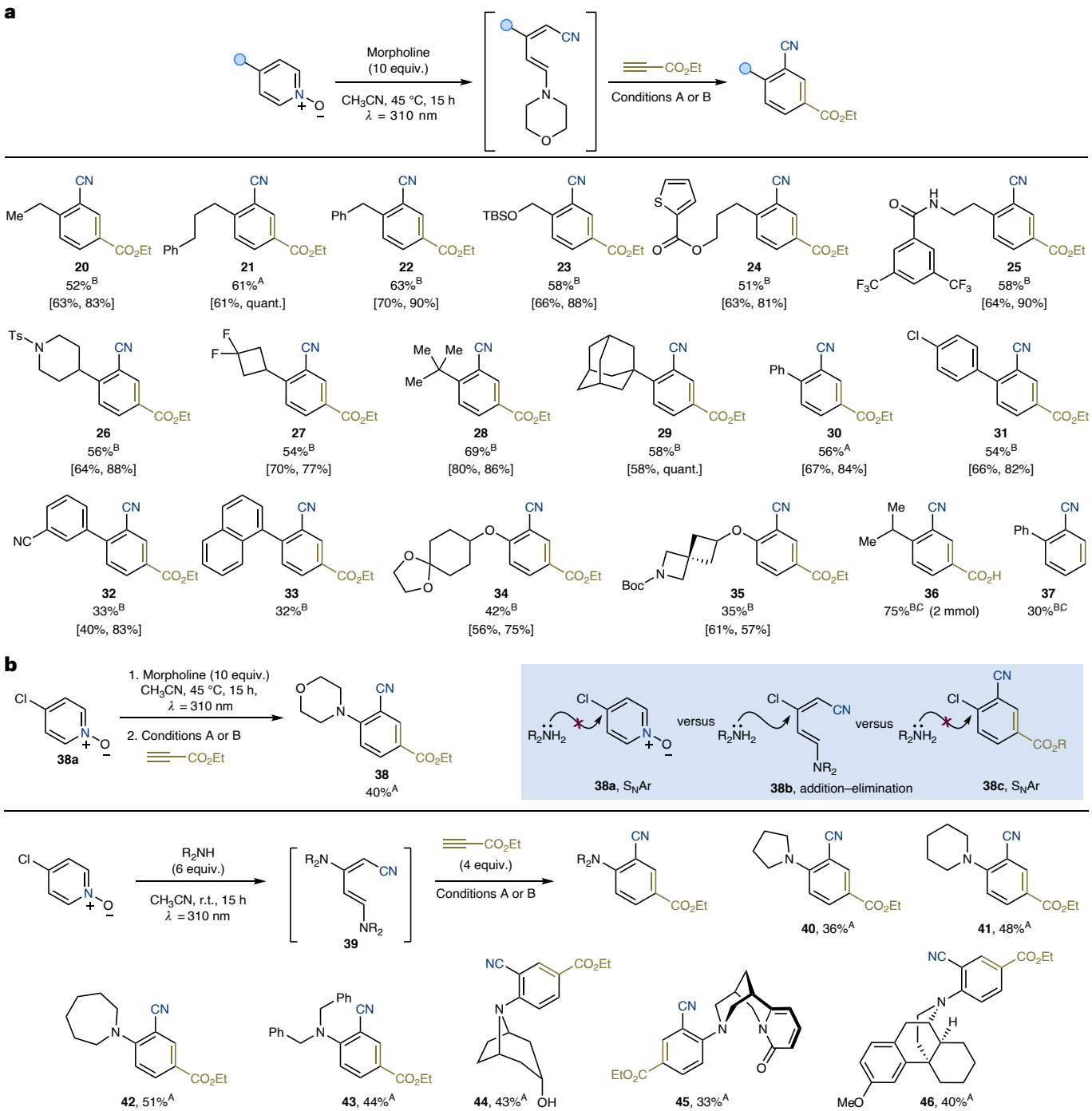

Fig. 4 | Scope for the pyridine-to-benzonitrile replacement. a, Pyridine scope. **b**, Tandem pyridine deconstruction–amination–Diels–Alder reactivity to give *ortho*-aminated benzonitriles. [Yield of step 1 (ring opening), yield of step 2 (cycloaddition)]. Superscripts A and B indicate reactions performed using conditions A and B (see Fig. 2 for details); for details of superscript C, see Supplementary Information. TBS, *tert*-butyldimethylsilyl; Ts, *p*-toluenesulfonyl; Boc, *tert*-butoxycarbonyl.

aligned system truly went through a dynamically concerted asynchronous Diels–Alder process or a dynamically stepwise process, Born–Oppenheimer molecular dynamics were applied to a model system at a suitable transition state geometry[83–86] (Fig. 3e). After random initiation, the productive runs were shown to form $r(C_1–C_2) < 1.6$ Å on average in 37 fs; by contrast, the $r(C_3–C_4)$ bond occurred 198 fs later and one trajectory did not even form a bond after >1,000 fs. The smallest time gap between the two bond-forming processes found was 52 fs, which is at the upper timescale of a C–C bond vibration (30–60 fs)[87], hence we propose that the reaction occurs through a dynamic stepwise mechanism forming an entropic zwitterionic intermediate before cyclizing to the productive Diels–Alder adduct[85].

Scope of the process

Having identified suitable conditions for the ring opening of pyridine-*N*-oxides and subsequent benzonitrile construction, we sought to combine both reactions into a one-pot process, thereby avoiding the isolation of any synthetic intermediate. This was achieved

https://doi.org/10.1038/s44160-025-00759-x

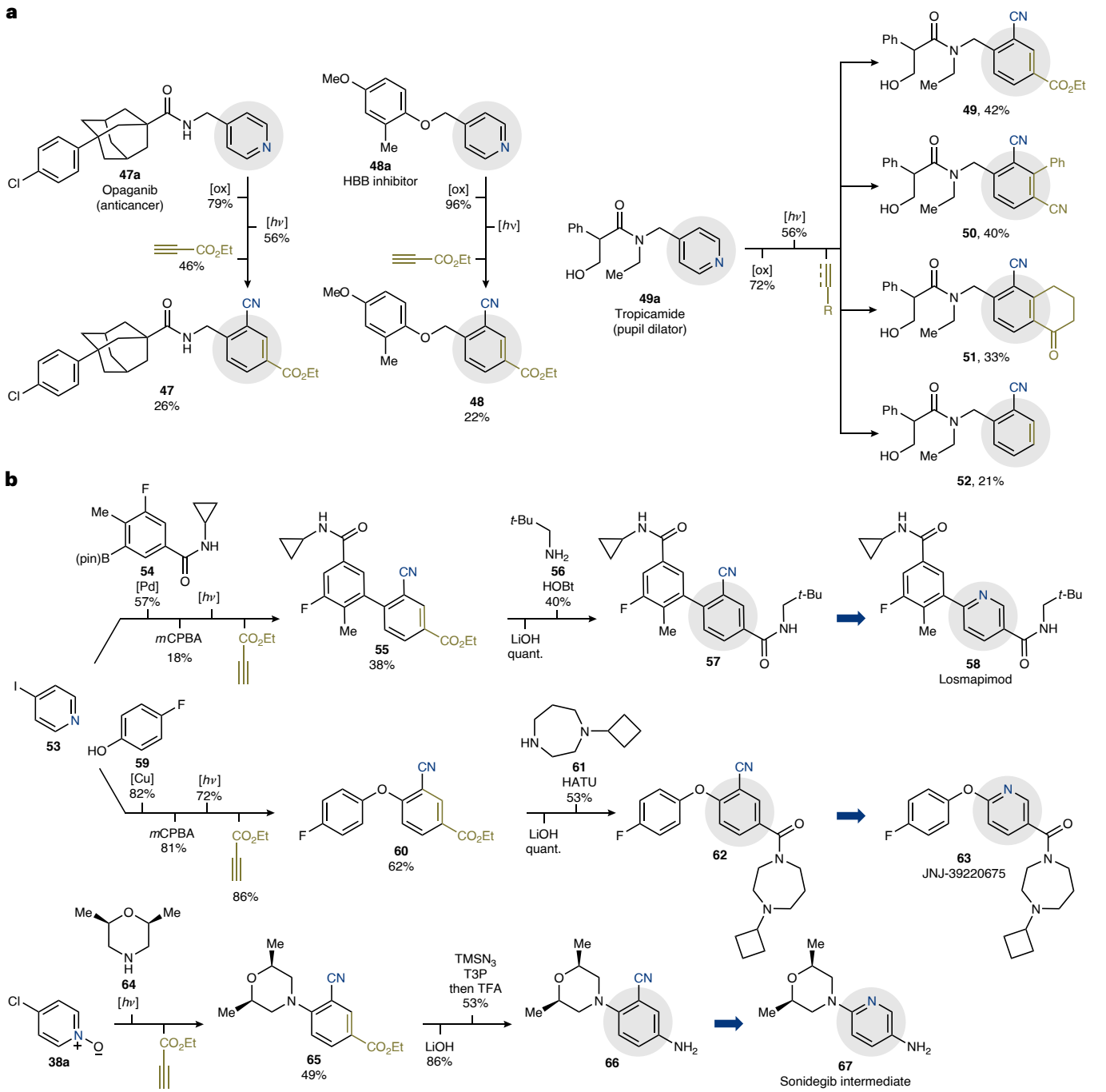

Fig. 5 | Application of the pyridine-to-benzonitrile replacement strategy to the synthesis of drug analogues. a, Use of the methodology for the late-stage pyridine-to-benzonitrile ring replacement of drugs. **b**, Use of the method for the preparation of 'unhappy water' analogues of pyridine drugs. B(pin), pinacol boronic ester; HATU, hexafluorophosphate azabenzotriazole tetramethyl uronium; T3P, propylphosphonic anhydride; $TMSN_3$, trimethylsilyl azide; TFA, trifluoroacetic acid. See Supplementary Information, section 11.5, for details of reaction conditions.

through directly telescoping both sets of reactions utilizing only evaporation of volatiles after the photochemical process to facilitate the switch in solvent and allow for the removal of the remaining morpholine (Fig. 4a).

We started scope exploration by first evaluating 4-alkyl pyridines. This enabled the use of primary groups (**20**–**25**) including derivatives with positions that are enthalpically (**22**, benzylic) or polarity (**24**, α-O) activated towards hydrogen-atom transfer[88,89]. This evaluation also demonstrated tolerance of silyl-protected alcohol (**23**), ester (**24**) and amide (**24**) functionalities. The reactivity was also extended to substrates containing secondary and tertiary alkyl substituents, such as a 4-*N*-Ts-piperidine (**26**) and a *gem*-difluoro-cyclobutane (**27**), and bulky *t*-Bu (**28**) and adamantyl (**29**) groups. It is interesting to note that many of these 4-alkyl-pyridine-*N*-oxides are accessed by straightforward Minisci reactivity[90–93]. This means that radical chemistry can be used as a stepping stone to functionalize in a selective manner the pyridine starting material for subsequent translation into the benzonitrile product. This offers valuable complementarity to the preparation of derivatives that would otherwise require C(sp^2)–C(sp^3) cross-couplings with transition metals[94,95].

4-Aryl groups were explored next, and the two-step one-pot cascade allowed for the synthesis of Ph (**30**), 4-Cl-C_6H_4 (**31**), 3-CN-C_6H_4 (**32**) and 1-naphthyl (**33**) containing biaryls.

Ortho-substituted benzonitrile ethers were prepared starting from 4-hydroxy-pyridine via a Mitsunobu reaction with secondary alcohols. Subsequent photochemical deconstruction and thermal cycloaddition gave **34** and **35** in good yield.

The scalability of the overall process was explored using 4-*i*-Pr-pyridine-*N*-oxide, which was converted in three telescoped steps (deconstruction, cycloaddition, ester hydrolysis) into the benzonitrile **36** on a 2-mmol scale in overall 75% yield. Furthermore, the use of **19a** could be adapted in the telescoped approach to give **37** in overall 30% yield.

An interesting outcome was obtained while extending this chemistry to 4-Cl-pyridine-*N*-oxide **38a**, which under the telescoped conditions delivered the 2-aminated benzonitrile **38** (Fig. 4b). Because **38a** is a commercial building block often used in nucleophilic aromatic substitution (S_NAr) chemistry, we initially reasoned that **38a** was undergoing in situ amination before ring opening en route to **38**. Alternatively, we hypothesized that morpholine expelled upon aromatization after the cycloaddition step might have resulted in a tandem Diels–Alder–S_NAr sequence. However, control experiments revealed that no S_NAr took place either with **38a** (45 °C) or **38c** (120 °C). This outcome is not surprising because these conditions are effectively base-free, which would limit the nucleophilic properties of the amine. Furthermore, several literature methods for S_NAr aminations were attempted **38c** and in all cases, the yield of the desired aminated benzonitrile did not exceed 14% (Supplementary Information, section 12, and Supplementary Table 17, entries 3–4). These observations suggested that ring opening occurred to generate chlorine-substituted aminopentadienenitrile **38b**, which undergoes addition–elimination with the amine to give **39** before Diels–Alder reactivity.

Recognizing the potential of this reactivity for tandem pyridine-to-benzonitrile conversion and *ortho*-amination, we explored the compatibility of the telescoped process with various amine coupling partners. Pleasingly, pyrrolidine (**40**), piperidine (**41**), azepane (**42**) and Bn_2NH (**43**) were tolerated, giving their constituent 2-aminobenzonitriles **40**–**43** in moderate to good yield. The ability of the strategy to deliver complex materials was further demonstrated by the arylation of alkaloid nortropine (**44**), the smoking cessant cytisine (**45**) and nor-dextromethorphan (**46**).

We believe this strategy for pyridine-to-benzonitrile ring replacement can have two main applications.

Considering the large number of pyridine-containing drugs, it can find use as a late-stage 'ring-replacer' to access new types of derivatives without the need for de novo individual synthesis, which is the current-state-of-the-art (Fig. 5a). This concept was showcased with the three-step modification of the anticancer opaganib (**47a**), the HBB inhibitor **48a** and the pupil dilator tropicamide (**49a**). These bioactive materials feature a 4-substituted pyridine core and underwent *N*-oxidation followed by photochemical deconstruction and thermal reconstruction with ethyl propiolate in overall good yields (**47**–**52**). In the case of **49a**, the photochemical step was run on a 0.3-mmol scale, which enabled parallel preparation of other derivatives (**49**, **50**, **51**) by changing the nature of the dienophile. We hope this can provide a powerful opportunity for library screening purposes by exploiting, in a modular manner, already established bioisosterism principles.

Furthermore, the alternative tactic for aromatic construction provided by this method can streamline the preparation of functionalized benzonitriles from unusual pyridine starting materials (Fig. 5b). We were keen to showcase this unique retrosynthetic opportunity and decided to prepare the 'unhappy water' benzonitrile analogues of pyridine-based losmapimod (**58**), JNJ-39220675 (**63**) and the key aniline fragment of sonidegib (**67**). The syntheses of **57** and **62** started from 4-iodopyridine **53** that underwent either Suzuki–Miyaura cross-coupling with **54** (three steps) or Ulmann coupling with phenol **59**. These steps provided access to 4-functionalized pyridines that were subjected to the three-step procedure for benzonitrile construction. Pleasingly, both derivatives were converted into **55** and **60**, respectively, in good yields. At this point, ester hydrolysis followed by amidation with either **56** or **61** provided the 'unhappy water' analogues **57** and **62** in five steps. The preparation of the sonidegib intermediate **67**, harnessed the tandem amination discussed above (Fig. 4b). Hence, commercial 4-chloropyridine-*N*-oxide **38a** was directly converted into the morpholine-containing derivative **65** in good yield. Subsequent hydrolysis and Curtius rearrangement led to aniline **66** in four steps. This highlights the versatility of the ester substituent which can be manipulated as a synthetic handle for further downstream functionalization in the synthesis of complex aromatic targets.

Conclusions

We have presented a method for the direct conversion of pyridines into benzonitriles. This strategy harnesses pyridine *N*-oxidation as an entry point for a photochemical event that deconstructs the azine into a nitrile-containing diene primed for Diels–Alder cycloaddition. The method displays a wide functional group tolerance allowing for the streamlined preparation of complex arene building blocks. We have demonstrated how this approach is amenable to the late-stage ring replacement of a variety of 4-substituted pyridine drug derivatives and allows for the rapid assembly of densely functionalized molecular libraries. We hope that the commercial availability of pyridines and the broad scope demonstrated here will make this strategy of use to industrial and academic end-users.

Methods

General procedure for the synthesis of aminopentadienenitriles

Pyridine-*N*-oxide (0.1 mmol, 1 equiv.) was added to a microwave vial, which was then capped with a Supelco aluminium crimp seal with a septum (PTFE/butyl), evacuated and purged with argon (×3). Degassed CH_3CN (5 ml, 0.02 M) was added followed by morpholine (88 µl, 1 mmol, 10 equiv.) and the solution was degassed with a stream of argon for 20 s. The microwave vial was then irradiated with 310 nm light in a Helios photoreactor for 15 h. The cap was then removed, and the solvent was evaporated to give a crude residue which was purified via column chromatography eluting on neutral Al_2O_3 to give the pure aminopentadienenitrile.

General procedure for the Diels–Alder cycloaddition

1 (27 mg, 0.1 mmol, 1 equiv.) was added to a microwave vial followed by dienophile (0.4 mmol, 4 equiv.), if solid. The vial was capped with a Supelco aluminium crimp seal with a septum (PTFE/butyl), evacuated and purged with argon (×3). Toluene (0.1 ml, 1 M) and dienophile (0.4 mmol, 4 equiv.), if liquid, were added. The sealed vial was then heated at 120 °C for 15 h. The cap was then removed, and the solvent was evaporated to give a crude residue which was purified via column chromatography eluting on silica gel to give the pure benzonitrile.

General procedure for one-pot arene synthesis

Step 1 (ring opening). Pyridine-*N*-oxide (0.1 mmol, 1 equiv.) was added to a microwave vial, which was then capped with a Supelco aluminium crimp seal with a septum (PTFE/butyl), evacuated and purged with argon (×3). Degassed CH_3CN (5 ml, 0.02 M) was added followed by morpholine (88 µl, 1 mmol, 10 equiv.) and the solution was degassed with a stream of argon for 20 s. The microwave vial was then irradiated with 310 nm light in a Helios photoreactor for 15 h. The cap was then removed, and the solvent was evaporated to give the crude aminopentadienenitrile which was dried under high vacuum to remove trace volatiles to give a crude residue which was used directly in the next step without further purification.

Step 2 (cycloaddition). To the crude aminopentadienenitrile from step 1, toluene (0.1 ml, 1 M) and ethyl propiolate (41 µl, 0.4 mmol, 4 equiv.) were added. The vial was capped with a microwave vial lid and the reaction was then heated in a microwave (µW) reactor at 150 °C for 2 h. The cap was then removed, and the solvent was evaporated to give a crude residue which was purified via column chromatography eluting on silica gel to give the pure benzonitrile.

Data availability

The authors declare that the data supporting the findings of this study are available within the paper and its Supplementary Information files.

References

1. Patani, G. A. & LaVoie, E. J. Bioisosterism: a rational approach in drug design. *Chem. Rev.* **96**, 3147–3176 (1996).
2. Hu, Y., Stumpfe, D. & Bajorath, J. Recent advances in scaffold hopping. *J. Med. Chem.* **60**, 1238–1246 (2017).
3. Subbaiah, M. A. M. & Meanwell, N. A. Bioisosteres of the phenyl ring: recent strategic applications in lead optimization and drug design. *J. Med. Chem.* **64**, 14046–14128 (2021).
4. Pearson, T. J. et al. Aromatic nitrogen scanning by ipso-selective nitrene internalization. *Science* **381**, 1474–1479 (2023).
5. Patel, S. C. & Burns, N. Z. Conversion of aryl azides to aminopyridines. *J. Am. Chem. Soc.* **144**, 17797–17802 (2022).
6. Eberle, L. & Ballmann, J. Synthesis of collidine from dinitrogen via a tungsten nitride. *J. Am. Chem. Soc.* **146**, 7979–7984 (2024).
7. Cheng, Q. et al. Skeletal editing of pyridines through atom-pair swap from CN to CC. *Nat. Chem.* **16**, 741–748 (2024).
8. Conboy, A. & Greaney, M. Synthesis of benzenes from pyridines via N to C switch. *Chem* **10**, 1940–1949 (2024).
9. Morofuji, T., Nagai, S., Watanabe, A., Inagawa, K. & Kano, N. Streptocyanine as an activation mode of amine catalysis for the conversion of pyridine rings to benzene rings. *Chem. Sci.* **14**, 485–490 (2023).
10. Morofuji, T., Kinoshita, H. & Kano, N. Connecting a carbonyl and a π-conjugated group through a *p*-phenylene linker by (5+1) benzene ring formation. *Chem. Commun.* **55**, 8575–8578 (2019).
11. Morofuji, T., Inagawa, K. & Kano, N. Sequential ring-opening and ring-closing reactions for converting *para*-substituted pyridines into I-substituted anilines. *Org. Lett.* **23**, 6126–6130 (2021).
12. Falcone, N., He, S., Hoskin, J., Mangat, S. & Sorensen, E. Nitrogen-to-carbon single atom point mutation of pyridine *N*-oxides. *Org. Lett.* **26**, 4280–4285 (2024).
13. Cabrera-Pardo, J. R., Chai, D. I., Liu, S., Mrksich, M. & Kozmin, S. A. Label-assisted mass spectrometry for the acceleration of reaction discovery and optimization. *Nat. Chem.* **5**, 423–427 (2013).
14. Uhlenbruck, B. J. H., Josephitis, C. M., de Lescure, L., Paton, R. S. & McNally, A. A deconstruction–reconstruction strategy for pyrimidine diversification. *Nature* **631**, 87–93 (2024).
15. Boswell, B. R., Zhao, Z., Gonciarz, R. L. & Pandya, K. M. Regioselective pyridine to benzene edit inspired by water-displacement. *J. Am. Chem. Soc.* **146**, 19660–19666 (2024).
16. Glorius, F. et al. Nitrogen-to-functionalized carbon atom transmutation of pyridine. *Chem. Sci.* **15**, 15205–15211 (2024).
17. De, S. et al. Pyridine: the scaffolds with significant clinical diversity. *RSC Adv.* **12**, 15385–15406 (2022).
18. Lazzara, P. R. & Moore, T. W. Scaffold-hopping as a strategy to address metabolic liabilities of aromatic compounds. *RSC Medicinal Chemistry* **11**, 18–29 (2020).
19. Patrick, G. L. *An Introduction to Medicinal Chemistry* 5th edn (Oxford University Press, 2013).
20. Pennington, L. D. & Moustakas, D. T. The necessary nitrogen atom: a versatile high-impact design element for multiparameter optimization. *J. Med. Chem.* **60**, 3552–3579 (2017).
21. Pennington, L. D., Collier, P. N. & Comer, E. Harnessing the necessary nitrogen atom in chemical biology and drug discovery. *Med. Chem. Res.* **32**, 1278–1293 (2023).
22. Vitaku, E., Smith, D. T. & Njardarson, J. T. Analysis of the structural diversity, substitution patterns, and frequency of nitrogen heterocycles among US FDA approved pharmaceuticals. *J. Med. Chem.* **57**, 10257–10274 (2014).
23. Ertl, P. Craig plot 2.0: an interactive navigation in the substituent bioisosteric space. *J. Cheminform.* **12**, 8 (2020).
24. Mowbray, C. E. et al. Pyrazole NNRTIs 3: optimisation of physicochemical properties. *Bioorg. Med. Chem. Lett.* **19**, 5603–5606 (2009).
25. Kaneko, K. et al. Studies on the metabolic fate of loprinone hydrochloride (1): blood level, distribution, metabolism, excretion after a single intravenous administration to rats. *Drug Metab. Pharmacokinet.* **9**, 149–162 (1994).
26. Ziemniak, J. A., Wynn, R. J., Aranda, J. V., Zarowitz, B. J. & Schentag, J. J. The pharmacokinetics and metabolism of cimetidine in neonates. *Dev. Pharmacol. Ther.* **7**, 30–38 (2017).
27. Fleming, F. F., Yao, L., Ravikumar, P. C., Funk, L. & Shook, B. C. Nitrile-containing pharmaceuticals: efficacious roles of the nitrile pharmacophore. *J. Med. Chem.* **53**, 7902–7917 (2010).
28. Ertl, P., Altmann, E., Racine, S. & Lewis, R. Ring replacement recommender: ring modifications for improving biological activity. *Eur. J. Med. Chem.* **238**, 114483 (2022).
29. Adams Jan Antoinette Cusi, R. et al. HSD17B13 inhibitors and/or degraders. WO patent WO 2024/075051 A1 (2024).
30. Klein, M. et al. Structure-based optimization and discovery of M3258, a specific inhibitor of the immunoproteasome subunit LMP7 (β5i). *J. Med. Chem.* **64**, 10230–10245 (2021).
31. Huang, J. et al. Discovery of a novel series of imipridone compounds as *Homo sapiens* caseinolytic protease P agonists with potent antitumor activities in vitro and in vivo. *J. Med. Chem.* **65**, 7629–7655 (2022).
32. Liu, M. et al. Discovery of novel aryl carboxamide derivatives as hypoxia-inducible factor 1α signaling inhibitors with potent activities of anticancer metastasis. *J. Med. Chem.* **62**, 9299–9314 (2019).
33. Ghisaidoobe, A. T. et al. Identification and development of biphenyl substituted iminosugars as improved dual glucosylceramide synthase/neutral glucosylceramidase inhibitors. *J. Med. Chem.* **57**, 9096–9104 (2014).
34. Tsou, H.-R. et al. Optimization of 6,7-disubstituted-4-(arylamino)-quinoline-3-carbonitriles as orally active, irreversible inhibitors of human epidermal growth factor receptor-2 kinase activity. *J. Med. Chem.* **48**, 1107–1131 (2005).
35. Wissner, A. et al. 4-Anilino-6,7-dialkoxyquinoline-3-carbonitrile inhibitors of epidermal growth factor receptor kinase and their bioisosteric relationship to the 4-anilino-6,7-dialkoxyquinazoline inhibitors. *J. Med. Chem.* **43**, 3244–3256 (2000).
36. Chen, J. M., Xu, S. L., Wawrzak, Z., Basarab, G. S. & Jordan, D. B. Structure-based design of potent inhibitors of scytalone dehydratase: displacement of a water molecule from the active site. *Biochemistry* **37**, 17735–17744 (1998).
37. Gunby, R. H. et al. Structural insights into the ATP binding pocket of the anaplastic lymphoma kinase by site-directed mutagenesis, inhibitor binding analysis, and homology modeling. *J. Med. Chem.* **49**, 5759–5768 (2006).
38. Boschelli, H. D. 4-Anilino-3-quinolinecarbonitriles: an emerging class of kinase inhibitors. *Curr. Top. Med. Chem.* **2**, 1051–1063 (2002).
39. Liu, C. et al. 5-Cyanopyrimidine derivatives as a novel class of potent, selective, and orally active inhibitors of p38α MAP kinase. *J. Med. Chem.* **48**, 6261–6270 (2005).

40. Neetha, M., Afsina, C. M. A., Aneeja, T. & Anilkumar, G. Recent advances and prospects in the palladium-catalyzed cyanation of aryl halides. *RSC Adv.* **10**, 33683–33699 (2020).
41. Hossaini, Z., Rostami-Charati, F., Sheikholeslami-Farahani, F. & Ghasemian, M. Synthesis of functionalized benzene using Diels–Alder reaction of activated acetylenes with synthesized phosphoryl-2-oxo-2H-pyran. *Z. Naturforsch. B* **70**, 355–360 (2015).
42. Kozmin, S. A., Janey, J. M. & Rawal, V. H. 1-Amino-3-siloxy-1,3-butadienes: highly reactive dienes for the Diels–Alder reaction. *J. Org. Chem.* **64**, 3039–3052 (1999).
43. Dai, M. et al. Highly selective Diels–Alder reactions of directly connected enyne dienophiles. *J. Am. Chem. Soc.* **129**, 645–657 (2007).
44. Koike, T., Tanabe, M., Takeuchi, N. & Tobinaga, S. Aminodienylesters. I: The cycloaddition reactions of *tert*-aminodienylester with α,β-unsaturated carbonyl compounds, styrenes, and quinones. *Chem. Pharm. Bull.* **45**, 243–248 (1997).
45. Hilt, G. & Smolko, K. I. Alkynylboronic esters as efficient dienophiles in cobalt-catalyzed Diels–Alder reactions. *Angew. Chem. Int. Ed.* **42**, 2795–2797 (2003).
46. Hilt, G. & Danz, M. Regioselective cobalt-catalyzed Diels–Alder Reaction towards 1,3-disubstituted and 1,2,3-trisubstituted benzene derivatives. *Synthesis* **2008**, 2257–2263 (2008).
47. Finsen, L., Becher, J., Buchardt, O., Koganty, R. R. & Enzell, C. R. Derivatives and reactions of glutaconaldehyde. XI. *N*-substituted 5-amino-2,4-pentadienenals, their oximes, and 5-amino-2,4-pentadienenitriles. Structural analysis by ^{1}H and ^{13}C NMR spectroscopy. *Acta Chem. Scand.* **34b**, 513–518 (1980).
48. Becher, J., Finsen, L., Winckelmann, I., Rao Koganty, R. & Buchardt, O. Derivatives and reactions of glutaconaldehyde—XII: Photochemical and thermal preparation of 5-amino-2,4-pentadienenitriles. *Tetrahedron* **37**, 789–793 (1981).
49. Weber, H. & Rohn, T. 2*H*-Azirine und 2-(ω-Cyanalkyl)furane als neuartige Photoprodukte aus [*n*](2,6)Pyridinophan-*N*-oxiden und ihre Bedeutung für den Reaktionsverlauf. *Chem. Ber.* **122**, 945–950 (1989).
50. Ma, J. et al. Detection and identification of reaction intermediates in the photorearrangement of pyridazine *N*-oxide: discrepancies between experiment and theory. *J. Org. Chem.* **84**, 10032–10039 (2019).
51. Lohse, C. Primary photoprocesses in isoquinoline *N*-oxides. *J. Chem. Soc. Perkin Trans.* **2**, 229–233 (1972).
52. Nakagawa, M., Kaneko, T. & Yamaguchi, H. Photoinduced oxidation of tryptamine derivatives. Formation of pyrrolo[2,3-*b*] indole and N^{b}-(4-cyanobutadienyl)tryptamine. *Chem. Commun.* **1972**, 603–604 (1972).
53. Nakagawa, M., Kaneko, T., Yamaguchi, H., Kawashima, T. & Hino, T. Photoinduced oxygenation of tryptamines by aromatic amine *N*-oxides. *Tetrahedron* **30**, 2591–2600 (1974).
54. Albini, A. & Alpegiani, M. The photochemistry of the *N*-oxide function. *Chem. Rev.* **84**, 43–71 (1984).
55. Lohse, C., Hagedorn, L., Albini, A. & Fasani, E. Photochemistry of pyridine *N*-oxides. *Tetrahedron* **44**, 2591–2600 (1988).
56. Hurlow, E. E. et al. Photorearrangement of [8]-2,6-pyridinophane *N*-oxide. *J. Am. Chem. Soc.* **142**, 20717–20724 (2020).
57. Shields, D. J. et al. Cracking under internal pressure: photodynamic behavior of vinyl azide crystals through N_2 release. *J. Am. Chem. Soc.* **142**, 18565–18575 (2020).
58. Türck, U. & Behringer, H. Zur Reaktion von Acetylenen mit Stickstoffwasserstoffsäure. Isoxazole aus Acetylenketonen. *Chem. Ber.* **98**, 3020–3024 (1965).
59. Moore, H. W., Hernandez, L. & Sing, A. Chlorocyanoketene. A new β-lactam synthesis. *J. Am. Chem. Soc.* **98**, 3728–3730 (1976).
60. Moore, H. W., Hernandez, L. Jr., Kunert, D. M., Mercer, F. & Sing, A. A new synthetic route to 2-azetidinones. Ring contraction of 4-azido-2-pyrrolinones to 3-cyano-2-azetidinones. *J. Am. Chem. Soc.* **103**, 1769–1777 (1981).
61. Nilova, A., Campeau, L.-C., Sherer, E. C. & Stuart, D. R. Analysis of benzenoid substitution patterns in small molecule active pharmaceutical ingredients. *J. Med. Chem.* **63**, 13389–13396 (2020).
62. Candish, L., Teders, M. & Glorius, F. Transition-metal-free, visible-light-enabled decarboxylative borylation of aryl *N*-hydroxyphthalimide esters. *J. Am. Chem. Soc.* **139**, 7440–7443 (2017).
63. Cheng, W.-M., Shang, R., Zhao, B., Xing, W.-L. & Fu, Y. Isonicotinate ester catalyzed decarboxylative borylation of (hetero)aryl and alkenyl carboxylic acids through *N*-hydroxyphthalimide esters. *Org. Lett.* **19**, 4291–4294 (2017).
64. Murarka, S. *N*-(Acyloxy)phthalimides as redox-active esters in cross-coupling reactions. *Adv. Synth. Catal.* **360**, 1735–1753 (2018).
65. Sugihara, H., Ukawa, K., Kuriki, H., Nishikawa, M. & Sanno, Y. Syntheses and β-adrenoceptor activities of 2-alkylamino-6-hydroxy-5-hydroxymethyl-1,2,3,4-tetrahydro-1-naphthalenols. *Chem. Pharm. Bull.* **25**, 2988–3002 (1977).
66. Sugihara, H., Watanabe, M., Motohashi, M., Nishikawa, M. & Sanno, Y. Aminotetralols. US patent US 4035512 A (1977).
67. Nokami, J., Ueta, K. & Okawara, R. Pyrolysis of β-hydroxy sulfoxides. II. Synthesis of allylic alcohols. *Tetrahedron Lett.* **19**, 4903–4904 (1978).
68. Paquette, L. A., Moerck, R. E., Harirchian, B. & Magnus, P. D. Use of phenyl vinyl sulfoxide as an acetylene equivalent in Diels–Alder cycloadditions. *J. Am. Chem. Soc.* **100**, 1597–1599 (1978).
69. Ess, D. H. & Houk, K. N. Distortion/interaction energy control of 1,3-dipolar cycloaddition reactivity. *J. Am. Chem. Soc.* **129**, 10646–10647 (2007).
70. Ess, D. H. & Houk, K. N. Theory of 1,3-dipolar cycloadditions: distortion/interaction and frontier molecular orbital models. *J. Am. Chem. Soc.* **130**, 10187–10198 (2008).
71. Fernández, I. & Bickelhaupt, F. M. Alder-ene reaction: aromaticity and activation-strain analysis. *J. Comput. Chem.* **33**, 509–516 (2012).
72. Wolters, L. P. & Bickelhaupt, F. M. The activation strain model and molecular orbital theory. *Wiley Interdiscip. Rev. Comput. Mol. Sci.* **5**, 324–343 (2015).
73. Bickelhaupt, F. M. & Houk, K. N. Analyzing reaction rates with the distortion/interaction-activation strain model. *Angew. Chem. Int. Ed.* **56**, 10070–10086 (2017).
74. Chandra Mallojjala, S. et al. Mechanism and origin of remote stereocontrol in the organocatalytic enantioselective formal C(sp^2)–H alkylation using nitroalkanes as alkylating agents. *J. Am. Chem. Soc.* **144**, 17399–17406 (2022).
75. Wheeler, S. E. Local nature of substituent effects in stacking interactions. *J. Am. Chem. Soc.* **133**, 10262–10274 (2011).
76. Wheeler, S. E. & Houk, K. N. Substituent effects in the benzene dimer are due to direct interactions of the substituents with the unsubstituted benzene. *J. Am. Chem. Soc.* **130**, 10854–10855 (2008).
77. Wheeler, S. E., McNeil, A. J., Müller, P., Swager, T. M. & Houk, K. N. Probing substituent effects in aryl–aryl interactions using stereoselective Diels–Alder cycloadditions. *J. Am. Chem. Soc.* **132**, 3304–3311 (2010).
78. Gonzalez-James, O. M., Kwan, E. E. & Singleton, D. A. Entropic intermediates and hidden rate-limiting steps in seemingly concerted cycloadditions. observation, prediction, and origin of an isotope effect on recrossing. *J. Am. Chem. Soc.* **134**, 1914–1917 (2012).
79. Yang, Z. et al. Mechanisms and dynamics of reactions involving entropic intermediates. *Trends in Chemistry* **1**, 22–34 (2019).

80. Knizia, G. Intrinsic atomic orbitals: an unbiased bridge between quantum theory and chemical concepts. *J. Chem. Theory Comput.* **9**, 4834–4843 (2013).
81. Knizia, G. & Klein, J. E. M. N. Electron flow in reaction mechanisms—revealed from first principles. *Angew. Chem. Int. Ed.* **54**, 5518–5522 (2015).
82. O'Ferrall, R. A. M. Relationships between E2 and E1cB mechanisms of β-elimination. *J. Chem. Soc. B* **1970**, 274–277 (1970).
83. Tan, J. S. J., Hirvonen, V. & Paton, R. S. Dynamic intermediates in the radical cation Diels–Alder cycloaddition: lifetime and suprafacial stereoselectivity. *Org. Lett.* **20**, 2821–2825 (2018).
84. Murakami, T. et al. Molecular dynamics simulation study of post-transition state bifurcation: a case study on the ambimodal transition state of dipolar/Diels–Alder cycloaddition. *J. Phys. Org. Chem.* **37**, e4611 (2024).
85. Black, K., Liu, P., Xu, L., Doubleday, C. & Houk, K. N. Dynamics, transition states, and timing of bond formation in Diels–Alder reactions. *Proc. Natl Acad. Sci. USA* **109**, 12860–12865 (2012).
86. Hase, W. L., Kihyung, S. & Gordon, M. S. Direct dynamics simulations. *Comput. Sci. Eng.* **5**, 36–44 (2003).
87. Levine, R. D. *Molecular Reaction Dynamics* (Cambridge Univ. Press, 2009).
88. Xu, H. J. et al. Radical mechanism in the photoinduced oxygen transfer from acridine *N*-oxides to cyclohexene. *J. Photochem. Photobiol. A* **48**, 53–59 (1989).
89. Petrosyan, A., Hauptmann, R. & Pospech, J. Heteroarene *N*-oxides as oxygen source in organic reactions. *Eur. J. Org. Chem.* **2018**, 5237–5252 (2018).
90. Choi, J., Laudadio, G., Godineau, E. & Baran, P. S. Practical and regioselective synthesis of C-4-alkylated pyridines. *J. Am. Chem. Soc.* **143**, 11927–11933 (2021).
91. Tan, C.-Y., Kim, M., Park, I., Kim, Y. & Hong, S. Site-selective pyridine C–H alkylation with alcohols and thiols via single-electron transfer of frustrated Lewis pairs. *Angew. Chem. Int. Ed.* **61**, e202213857 (2022).
92. Choi, H., Mathi, G. R., Hong, S. & Hong, S. Enantioselective functionalization at the C4 position of pyridinium salts through NHC catalysis. *Nat. Commun.* **13**, 1776 (2022).
93. Lee, W., Jung, S., Kim, M. & Hong, S. Site-selective direct C–H pyridylation of unactivated alkanes by triplet excited anthraquinone. *J. Am. Chem. Soc.* **143**, 3003–3012 (2021).
94. Zhang, P., Le, C. C. & MacMillan, D. W. C. Silyl radical activation of alkyl halides in metallaphotoredox catalysis: a unique pathway for cross-electrophile coupling. *J. Am. Chem. Soc.* **138**, 8084–8087 (2016).
95. Huihui, K. M. M. et al. Decarboxylative cross-electrophile coupling of *N*-hydroxyphthalimide esters with aryl iodides. *J. Am. Chem. Soc.* **138**, 5016–5019 (2016).

Acknowledgements

D.L. acknowledges the European Research Council for a grant (101086901); H.P.C. acknowledges AstraZeneca for a PhD Case Award; N.K. acknowledges the Fonds der Chemischen Industrie for a Kekulé fellowship. C. Vermeeren is kindly acknowledged for help in the purification of some of the materials. Computational calculations were performed with computing resources granted by RWTH Aachen University under project RWTH1268 and computational facilities of the Advanced Computing Research Centre, University of Bristol.

Author contributions

H.P.C., A.R. and D.L. designed and supervised the project. H.P.C., R.G., N.K. and C.S. performed all the synthetic work. M.J.T. performed all the computational work. R.G., N.K., C.S., M.J.T., O.T., A.R., H.P.C. and D.L. analysed the results and wrote the manuscript.

Funding

Open access funding provided by RWTH Aachen University.

Competing interests

The authors declare no competing interests.

Additional information

Supplementary information The online version contains supplementary material available at https://doi.org/10.1038/s44160-025-00759-x.

Correspondence and requests for materials should be addressed to Alessandro Ruffoni, Henry P. Caldora or Daniele Leonori.

Peer review information *Nature Synthesis* thanks Benjamin Boswell, Xiao-Song Xue and the other, anonymous, reviewer(s) for their contribution to the peer review of this work. Primary Handling Editor: Thomas West, in collaboration with the *Nature Synthesis* team.